

A Deep Learning Based Approach for Response Prediction of Beam-like Structures

Tianyu Wang¹, Wael A. Altabay^{1,2}, Mohammad Noori^{3,*} and Ramin Ghiasi¹

¹International Institute for Urban Systems Engineering, Southeast University, Nanjing, 210096, China

²Department of Mechanical Engineering, Faculty of Engineering, Alexandria University, Alexandria, 21544, Egypt

³Department of Mechanical Engineering, California Polytechnic State University, San Luis Obispo, CA, 93405, USA

*Corresponding Author: Mohammad Noori. Email: mnoori52@yahoo.com

Received: 18 April 2020; Accepted: 21 August 2020

Abstract: Beam-like structures are a class of common but important structures in engineering. Over the past few centuries, extensive research has been carried out to obtain the static and dynamic response of beam-like structures. Although building the finite element model to predict the response of these structures has proven to be effective, it is not always suitable in all the application cases because of high computational time or lack of accuracy. This paper proposes a novel approach to predict the deflection response of beam-like structures based on a deep neural network and the governing differential equation of Euler-Bernoulli beam. The Prandtl-Ishlinskii model is introduced as an element of prediction model to simulate the plasticity of this beam structure. Finally the application of the proposed approach is demonstrated through four numerical examples including linear elastic/ideal plastic beam under concentrated/sinusoidal load and elastic/plastic continuous beam under seismic load to demonstrate a proof of concept for the effectiveness of this AI-based approach.

Keywords: Beam-like structure; surrogate model; deep neural network; Prandtl-Ishlinskii model

1 Introduction

As an important structural member, beam has been studied for over several centuries. A large number of classic and fundamental studies on beam analysis have been reported in the literature including in traditional steel structures [1], concrete structures [2–9], nano materials [10–14], and functionally graded materials [15], to cite a few examples. Beams are also used as the simplified model for some complex structures, such as bridge structures [16–21], chimney structures [22], and tall buildings [23]. Therefore, a large number of methods have been proposed to obtain the static and dynamic response of beam-like structures. Analytical method for beam analysis is a traditional approach which is still commonly used. This method can be used to obtain the exact solution for the deflection or stress analysis of beam structures, however, it can only be applied in static analysis. Finite element method (FEM), as the most widely used method, is a practical approach for this purpose, however, it requires discretization, mesh generation and an



This work is licensed under a Creative Commons Attribution 4.0 International License, which permits unrestricted use, distribution, and reproduction in any medium, provided the original work is properly cited.

iterative calculation, especially for materials with nonlinear force-displacement behavior. Nevertheless, for some situations that high accuracy of the results is not necessary, FEM, as a faster response prediction method of beam structure is a feasible solution. However, for large systems FEM is not an efficient approach and is time consuming. As an alternative approach, surrogate model is a type of approximate mathematical modeling that can be used to describe or predict important response properties of a real structure. Given the advantage of low computational cost, surrogate models have been widely applied in several areas of engineering including structural optimization [24–27], reliability analysis [28–31], damage detection [32–43], processing big data collected from the structures sensor network [44], etc. For different application scenarios, different surrogate models have been proposed. The common models include: polynomial response surface models [45,46], Kriging model [47–49], neural network model [50–56]. Neural networks, in particular, because of their powerful and universal approximation capability [57,58], are widely used as a valid surrogate model.

In structural response prediction area, neural network is also a useful tool. The properties of neural networks make it possible to describe and model dynamic systems. Early in 1993, Masri et al. [59] used a multilayer perceptron (MLP) with three hidden layers to identify the Duffing oscillator. Later, He, Wu and their co-workers used a back-propagation (BPNN) neural network and self-recurrent neural network (SRNN) in response prediction of linear elastic structures [60–62]. Joghataie et al. [63] introduced the Prandtl–Ishlinskii operator [64] into FFNN as the hidden layer and proposed the Prandtl neural network (PNN) to predict the dynamic response of systems with hysteresis. Lagaros and Papadrakakis [65] used neural networks to predict the seismic response of a nonlinear three-dimensional building. With the development of powerful computer technology, many researchers focused their research on deep learning [66,67]. Deep learning models are regarded as a special form of neural network model and have been used in response prediction [68].

Although a large number of researchers have already focused on neural network based response prediction of dynamic systems, most neural network based models are a black-box model [69]. That means the network cannot capture the complex dynamic characteristics of most systems. In addition, black box neural networks are not suited or reliable for most engineering applications and for adaptation in surrogate models. Another drawback of these models is the need for a large volume of data to train them. In order to develop an alternative approach, such as a white-box model or gray-box model for development of surrogate models, some researchers have proposed direct utilization of neural networks for solving the governing differential equations (DE) of these systems [70–74].

Recently, deep learning, which is basically a network with multiple hidden layers of neurons, has also been applied in solving and identifying the ordinary and partial differential equations. Han et al. [75] used a deep learning method to solve a type of high order nonlinear differential equation. Sirignano et al. [76] proposed a strategy for improving Galerkin method by deep learning and introduced a deep learning based Galerkin method to solve partial differential equations. Wu et al. [77–79] proposed a physics-based machine learning method for solving hydrodynamic problems. Raissi et al. [80–84] utilized deep research in physics-based deep learning and demonstrated its potential applications by developing an automatic differential operator [85] and Runge-Kutta method [86]. Based on these recent developments and success in utilization of deep neural network, and given their unique capabilities, deep neural networks have the potential to be used for developing new types of surrogate models with high accuracy and robustness for the dynamic response of structural systems. In order to utilize these networks to develop an alternative, direct and efficient tool for the direct solution of structural dynamics problems, some fundamental research is needed.

In this paper, as a preliminary step towards the aforementioned goal, we introduce a new type of deep neural network based on the governing equations of Euler-Bernoulli beam to predict its deflection response.

Beams made of both elastic and plastic materials are taken into consideration. The plastic behavior of the material is regarded as a hysteretic behavior in the macro level and is modeled by Prandtl–Ishlinskii model. Finally, two numerical examples are presented to validate the effectiveness of the proposed method. The results are compared respectively with the modal superposition method and finite element method. As this study shows, within a certain accuracy, the proposed method is much faster than the conventional method. Therefore, the proposed approach offer a potentially significant alternative approach to be considered for engineering applications.

2 The Formulation of the Proposed Method

In this section the formulation of the proposed strategy is presented.

2.1 The Governing Equation of the Beam

The dynamic behavior of Euler-Bernoulli beam can be described by the following partial differential equation (PDF):

$$m \frac{\partial^2}{\partial t^2} w(x, t) + c \frac{\partial}{\partial t} w(x, t) + EI \frac{\partial^2}{\partial x^2} w(x, t) = f(x, t) \quad t \in [0, T], \quad x \in \Omega \quad (1)$$

where $w(x, t)$ is the deflection, m and c are the linear mass density and damping, EI is the bending stiffness and $f(x, t)$ is the excitation. Besides, we need the initial condition $w(x, 0) = w_0(x)$ and the boundary condition $w(x, t) = g(x, t) \quad x \in \partial\Omega$ to analyze the vibration of beam.

Similar to finite element method, for the solution of Eq. (1) $u(x, t)$ can be expressed as the combination of deflections at several discrete points and can be expressed as:

$$u(x, t) = \Phi \mathbf{w} \quad (2)$$

In Eq. (2), Φ and \mathbf{w} can be expressed as follows:

$$\Phi = [\phi_1(x) \quad \phi_2(x) \quad \dots \quad \phi_i(x) \quad \dots \quad \phi_m(x)] \quad (3)$$

$$\mathbf{w} = [w(x_1, t) \quad w(x_2, t) \quad \dots \quad w(x_i, t) \quad \dots \quad w(x_m, t)]^T \quad (4)$$

We call matrix Φ as the shape function vector. In order to satisfy Eq. (1), we construct the following objective function as:

$$J(x) = \|\Phi(x)\mathbf{w} - w(x, t)\|_{x \in \Omega, t \in [0, T]}^2 \quad (5)$$

The shape function vector $\Phi(x)$ is approximated by a deep neural network (ANN-1). If $J(x) = 0$, $u(x, t)$ is an exact solution of the governing partial differential Eq. (1). Therefore, the goal is to find a shape function vector $\Phi(x)$ that can minimize the error $J(x)$.

Let $x = x_i$ ($i = 1, 2, \dots, m$), thus, the following differential function set with an unknown function set $\mathbf{w} = [w(x_1, t) \quad w(x_2, t) \quad \dots \quad w(x_i, t) \quad \dots \quad w(x_m, t)]^T$ can be obtained:

$$\begin{aligned} & \begin{bmatrix} m(x_1) & \dots & 0 \\ \vdots & \ddots & \vdots \\ 0 & \dots & m(x_n) \end{bmatrix} \begin{bmatrix} \ddot{w}(x_1, t) \\ \vdots \\ \ddot{w}(x_n, t) \end{bmatrix} + \begin{bmatrix} c(x_1) & \dots & 0 \\ \vdots & \ddots & \vdots \\ 0 & \dots & c(x_n) \end{bmatrix} \begin{bmatrix} \dot{w}(x_1, t) \\ \vdots \\ \dot{w}(x_n, t) \end{bmatrix} \\ & + \begin{bmatrix} EI(x_1)\phi''_1(x_1) & \dots & EI(x_1)\phi''_n(x_1) \\ \vdots & \ddots & \vdots \\ EI(x_n)\phi''_1(x_n) & \dots & EI(x_n)\phi''_n(x_n) \end{bmatrix} \begin{bmatrix} w(x_1, t) \\ \vdots \\ w(x_n, t) \end{bmatrix} = \begin{bmatrix} f(x_1, t) \\ \vdots \\ f(x_n, t) \end{bmatrix} \quad (6) \end{aligned}$$

When the time space t is discretized $[t_1, t_2, \dots, t_n]$ and $t_{i+1} = t_i + \Delta t$. The deflection response $w(x_1, t_{i+1}), w(x_2, t_{i+1}), \dots, w(x_n, t_{i+1})$ at coordinate $x = x_1, x_2, \dots, x_n$ can be predicted by a feed-forward neural network (ANN-2).

Therefore, the deflection response of the Euler-Bernoulli can be predicted by using a deep neural network with two sub-nets as in Fig. 1.

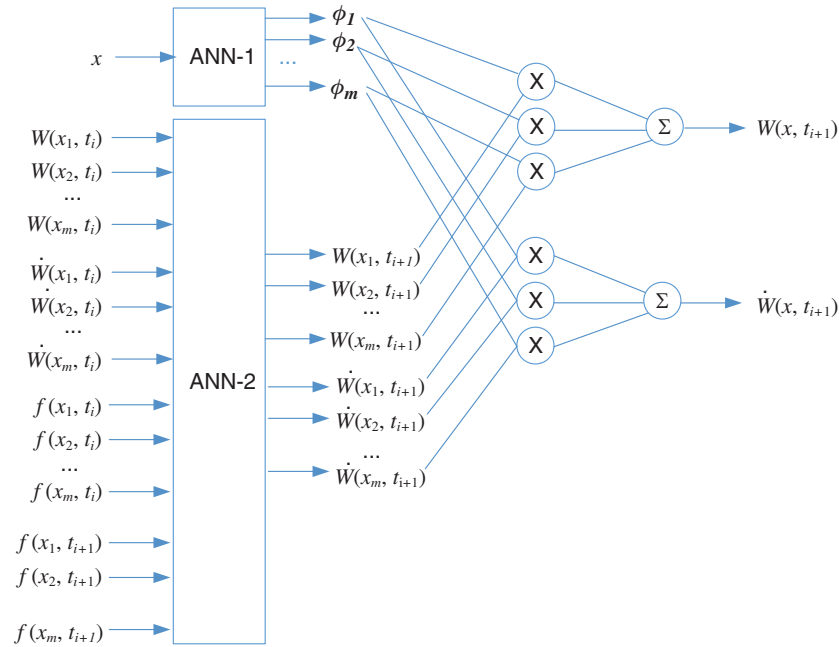


Figure 1: The architecture of the proposed neural network for the response prediction of beam

The deep neural network in Fig. 1 can be divided into two sub-nets as ANN-1 and ANN-2. ANN-1 is used to approximate the coefficient vector Φ , and ANN-2 predicts the response at the coordinates of x_1, x_2, \dots, x_m . Usually some nonlinear functions are used as the activation function to simulate the vibration of the beam, such as hyperbolic tangent function, logistic function as well as ReLU function or trigonometric function, etc. The number of hidden layers will also effect the prediction result of deep learning model. Generally speaking, the prediction precision will increase with the number of hidden layers. However, due to the limitation of computing power and the number of training samples, the number of hidden layers cannot increase infinitely. In real examples, we determine the number of hidden layers mainly from two aspects: First is the complexity of load distribution. The other is the material property of beam-like structure. In our research practice, the model of elastic structure is usually with 1-3 hidden layer while the model of plastic structure is with 3-5 hidden layer.

Prediction of beam deflection response can be described through the following steps:

1. **Data preparation:** Obtain the training data from an experiment, field test or numerical simulation when the beam is subjected to load $f_1(x, t)$. The following data are needed for the model training.

1) Sets 1: n_1 set of deflection response: $w(x_1, t_i), w(x_2, t_i), \dots, w(x_m, t_i), i = 1, 2, \dots, n_1$

2) Sets 2: n_2 set of deflection response: $(x, w(x_j, t_j)) j = 1, 2, \dots, n$, where $x_j \in [0, L]$ and L is the total length of the beam, and $t_j \in \{t_1, t_2, \dots, t_n\}$

2. **Model training:** We will use part of the data in sets 1 for training the artificial neural network without hidden layers for response prediction (ANN-2). And part of the data in sets 2 to train the deep neural network for function approximation (ANN-1).

3. **Model test:** The remaining part of data set 1 and set 2 can be used to test the trained model. If the model is well-trained, the predicted results by ANN-1 and ANN-2 will be close to the real value.

4. **Response prediction:** ANN-2 can be used to predict the response $w(x_1, t_i)$, $w(x_2, t_i)$, \dots , $w(x_m, t_i)$ under load $f_2(x, t)$. ANN-1 is used to predict the response $w(x, t_i)$ at any coordinate x along the beam. If the external excitation $f_2(x, t)$ and the initial condition are given, proposed deep neural network can be used to predict the deflection response of beam. Meanwhile, the angel and curvature response can also be obtained by calculating the numerical differentiation of deflection response.

2.2 Response Prediction of a Linear Elastic Beam

For an elastic beam, a linear network with several hidden layers can be used as a sub net of ANN-2. The number of layers are usually less than three. In this network, a linear function is used as the activation function for each layers. The architecture of sub net ANN-2 is presented in Fig. 2.

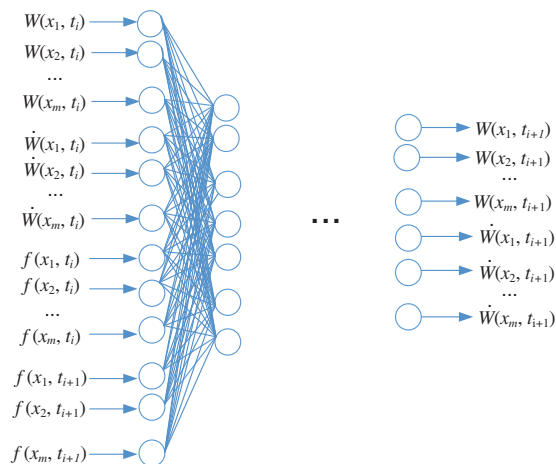


Figure 2: The architecture of ANN-2 for the response prediction of linear beam

2.3 Response Prediction of a Linear Elastic Beam

Plasticity is widely encountered in the displacement response of engineering structures. The plasticity of beam like structures usually manifests as hysteresis in macro level. Therefore, the following equation can be used to describe the bending deformation of plastic beam.

$$m(x) \frac{\partial^2}{\partial t^2} w(x, t) + c(x) \frac{\partial}{\partial t} w(x, t) + R(w'') = f(x, t) \quad (7)$$

where $R(w'')$ is the resilience, or the restoring force, a function related to curvature $w'' = \frac{\partial^2 w(x, t)}{\partial x^2}$, stiffness, coordinate x and time t . Similar to elastic beam, the deflection $w(x, t)$ can be written as the combination of the deflection at several points.

We introduce hysteresis in ANN-2 by using Prandtl-Ishlinskii model to build Prandtl neural network (PNN) [63]. Prandtl-Ishlinskii model is a hysteretic operator widely applied in controls engineering and can simulate the hysteretic system well. The Prandtl-Ishlinskii model can be expressed as:

$$y(\tau) = \int_0^R w(r) \varepsilon_r[x(\tau)] dr \quad (8)$$

where $y(\tau)$ is the output signal, $x(\tau)$ is the input signal, $w(r)$ is the density function and ε_r is the stop operator which is expressed in Eq. (9):

$$\varepsilon_r[x(0)] = e_r[x(0)] \quad (9)$$

$$\varepsilon_r[x(t)] = e_r[x(t) - x(t_i) + \varepsilon_r(t_i)] \quad (10)$$

where $e_r(x) = \min\{r, \max\{-r, x\}\}$, $t \in [t_i, t_{i+1}]$. And $x(t)$ should be a monotonic function in the section $[t_i, t_{i+1}]$. r is a parameter which defines the shape of hysteresis loop. Fig. 3 shows the hysteresis loop of the stop operator.

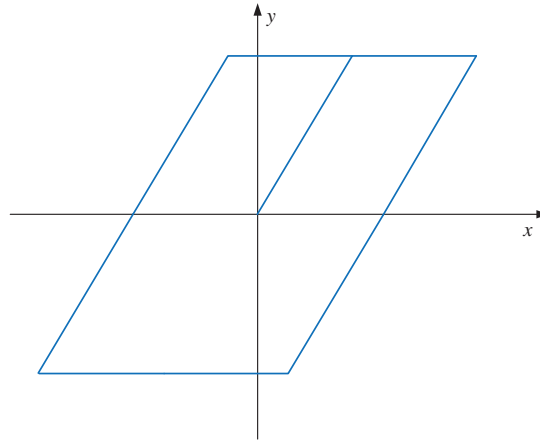


Figure 3: The hysteretic loop of the stop operator

If we approximate Eq. (8) as a sum of infinite terms, the following Eq. (9) can be obtained as:

$$y(\tau) = \sum_{i=1}^M w(r) \varepsilon_r[x(\tau)] \quad (11)$$

Therefore, the architecture of ANN-2 can be rebuilt as shown in Fig. 4. Compared with the network for a linear beam, the stop operator ε_{r_i} ($i = 1, 2$) is used as the activation function. r_1, r_2, \dots, r_M are the hyper-parameters of neural network and they can be determined by the following equation [87]:

$$r_i = \frac{i|x_{max}|}{M} \quad (12)$$

3 Numerical Examples

In this section, several numerical examples are presented for both linear and nonlinear cases. The first example simulates the linear dynamic response of a simply-supported elastic beam subjected to a concentrated force in the mid-span. We use the data from harmonic vibration as the training data. And the final result under triangular and rectangular periodic loads are compared with the result from the finite element model based on Newmark- β method. In the second examples, a simply-supported beam made of an ideal elasto-plastic material is presented. The third and fourth examples include a continuous beam under seismic load and the nonlinear dynamics of this beam with plastic deformation.

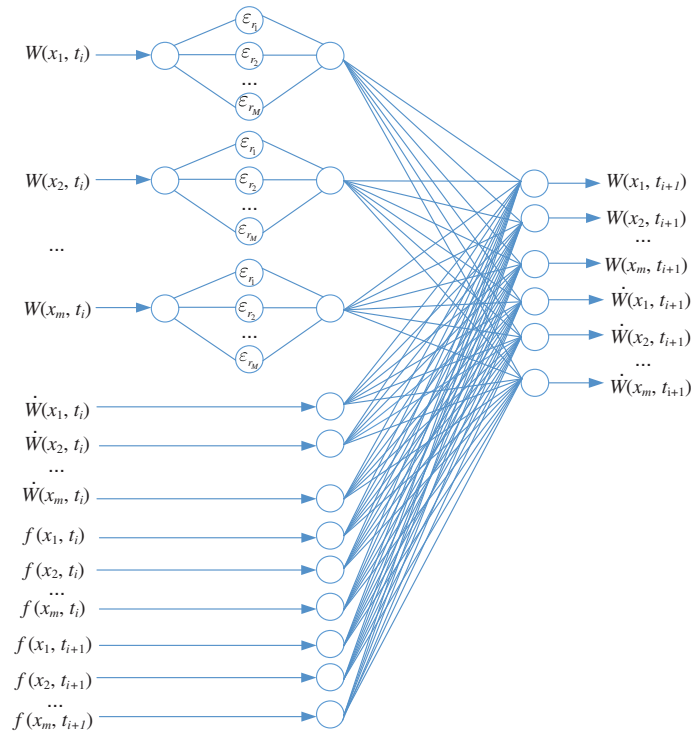


Figure 4: Architecture of ANN-2 for the response prediction of a nonlinear beam

The analysis result from the finite element model is calculated by ABAQUS and used to train the deep neural network model. The surrogate model is used to predict the nonlinear response of a bridge under seismic load.

3.1 Linear Vibration of an Elastic Beam

The length of beam L is 235 mm while the cross section is rectangular with a height of $h = 23$ mm and a width of $b = 7$ mm. The material density ρ is 2800 kg/m³ and the elastic modulus E is 72 GPa. The beam is subjected to a concentrated load on the mid-span as shown in Fig. 5.

For building the surrogate model to predict the deflection response of the beam, we will choose five points along the beam as $\{x_1, x_2, x_3, x_4, x_5\}$ and the corresponding deflections as $\{W(x_1, t), W(x_2, t), W(x_3, t), W(x_4, t), W(x_5, t)\}$. In this example, $x_1 = 0.1L$, $x_2 = 0.3L$, $x_3 = 0.5L$, $x_4 = 0.7L$, $x_5 = 0.9L$.

To obtain the training data, we assume the force term $f(t) = F \sin(\Omega t)$ and obtain the deflection response of different points as the training data. Where $F = 100N$ and $\Omega = 0.001\Omega$, ω_1 is the fundamental natural frequency of the beam. The training data of the deflection varies with time as shown in Fig. 6.

A multilayer perceptron with 5 hidden layers is used in this numerical example to approximate the shape function vector which describes the dynamic displacement of the beam as shown in Fig. 7. In the deep neural network, the sine function $\sin(x)$ is used as an activation function for each hidden layer.

To verify the effectiveness of the deep learning model to predict the response of a beam structure the response of the beam under a triangular and a rectangular periodic load are used in the examples. Fig. 8 shows the time history of these periodic loads. The response predictions are presented in Figs. 9 and 10 and compared with the results from finite element (FEM).

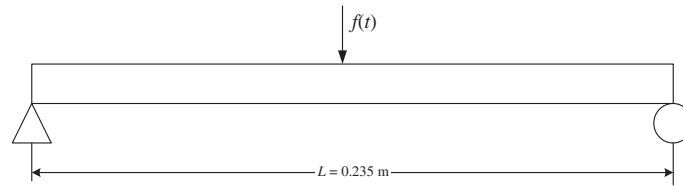


Figure 5: The force diagram of the simply-supported beam

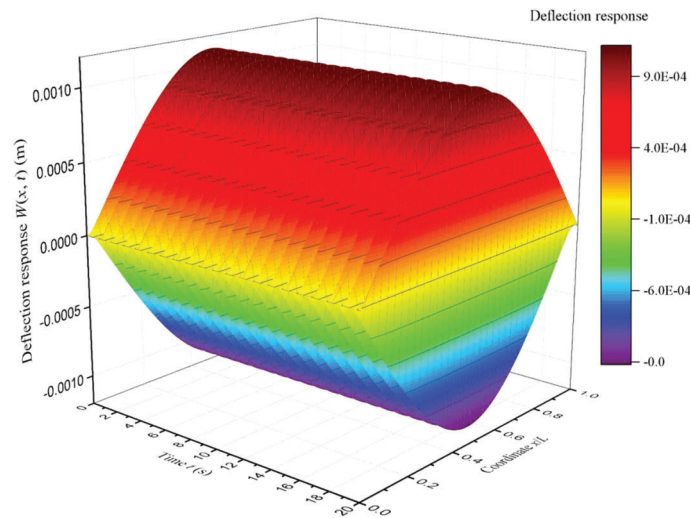


Figure 6: The training data of response prediction for example 1

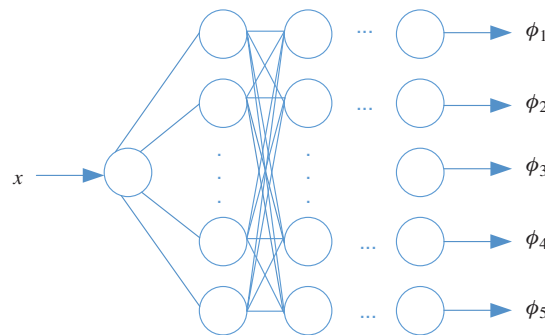


Figure 7: The ANN-1 for shape function approximation in example 1

3.2 Nonlinear Dynamic Response of a Plastic Beam

In this section, the dynamic response of an ideal elasto-plastic beam is presented as an example. The beam is simply-supported with the length $L = 2000$ mm and a rectangular cross section $A = 100$ mm \times 100 mm. The material characteristics are listed as: Elastic modulus $E = 200$ Gpa, and yield strength $f_y = 380$ Mpa. A sinusoidal load with a constant uniform amplitude $Q(t) = 7.5 \times 10^5 \sin \pi t$ is applied in the middle span as shown in Fig. 11.

Since it is difficult to obtain the exact solution for the vibration of a structure with plastic material behavior, we use a finite element model (FEM) by ABAQUS to obtain the training data and verify the response prediction. Rayleigh proportional damping matrix is used in the analysis, which is a linear

combination of stiffness matrix and mass matrix. The expression of Rayleigh damping can be written as: $\mathbf{C} = \alpha\mathbf{K} + \beta\mathbf{M}$. In this example, $\alpha = 3.0$ and $\beta = 0.0$. Because of the plasticity of the beam, we use a piecewise shape function to describe the dynamic displacement. Therefore, to make sure the shape coefficients $\phi_1, \phi_2 \dots, \phi_n$ are independent, we build a network with several sub-nets as in Fig. 12.

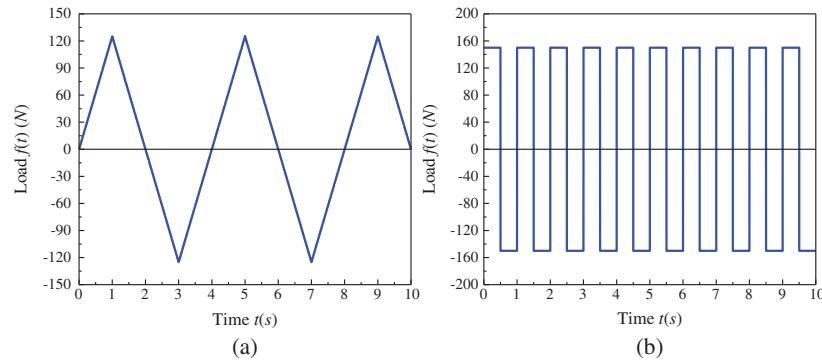


Figure 8: The test load to verify the deep learning model. (a) Triangular periodic load and (b) Step load

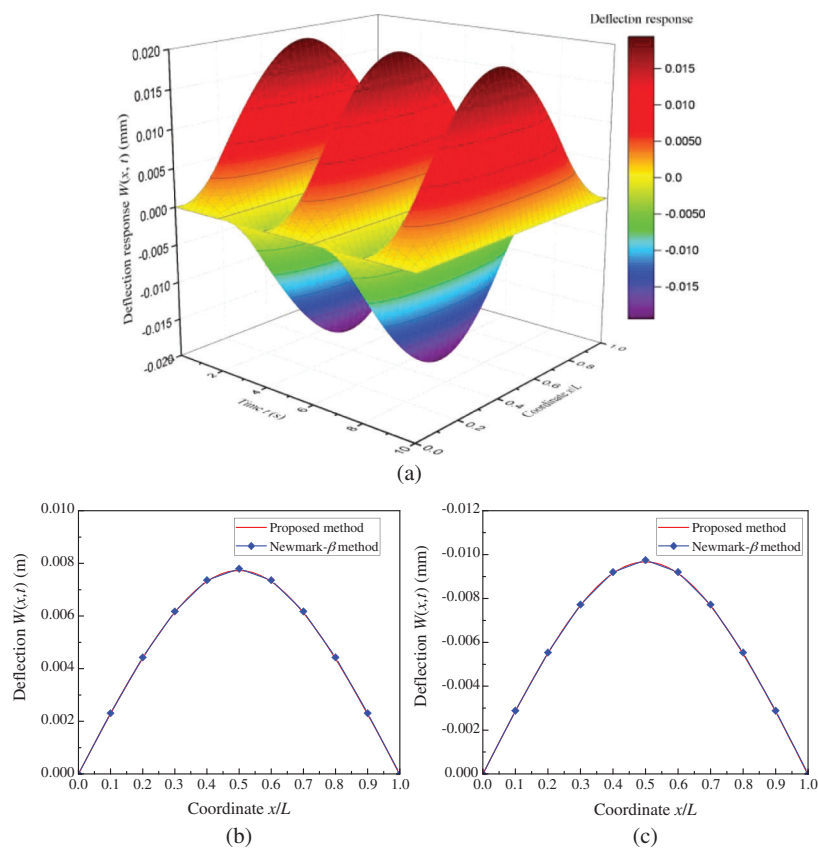


Figure 9: Response prediction under a triangular periodic load. (a) The 3D figures of the deflection as a function of time t and coordinate x under triangular periodic load, (b) The deflection of beam when $t = 0.4$ s and (c) The deflection of beam when $t = 6.5$ s

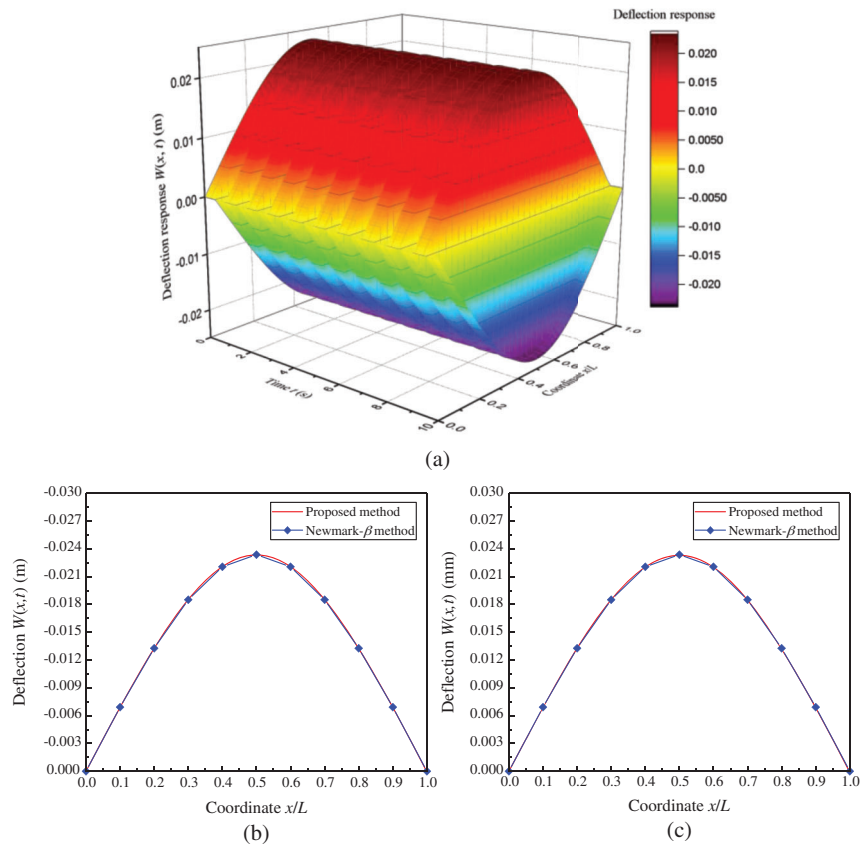


Figure 10: Response prediction under a rectangular periodic load. (a) The 3D figures of the deflection as a function of time t and coordinate x under a rectangular periodic load, (b) The deflection of beam at $t = 0.6$ s and (c) The deflection of beam at $t = 5.8$ s

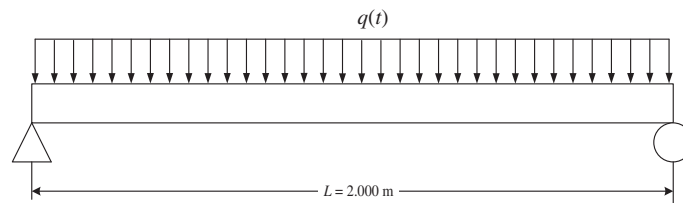


Figure 11: The force diagram of the plastic simply-supported beam

In this network, section the chosen function $F_{a,h}(x)$ is used as the first layer of the network which is defined as:

$$F_{ah}(x) = \begin{cases} 0 & x \in (-\infty, a - h) \\ x & x \in [a - h, a + h] \\ 0 & x \in (a + h, +\infty) \end{cases} \quad (13)$$

Every sub-net contains five hidden layers with the activation function $\sin(x)$ to approximate the shape coefficients.

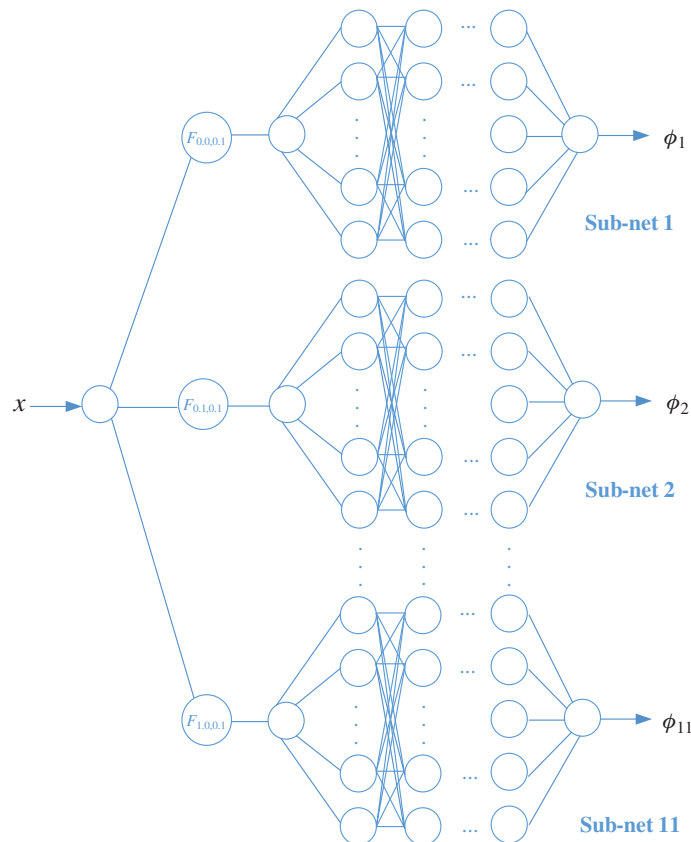


Figure 12: The ANN-1 for the shape function approximation in example 2

The training data are shown in Fig. 13 which gives the variation of the transverse deformation of beam as a function of time.

A multilayer perceptron with 5 hidden layers is used in each sub-net of the numerical example to approximate the shape function vector. Similar to the previous example, a sine function $\sin(x)$ is used as the activation function for each hidden layer.

Several different loads are applied to the deep learning model to verify the effectiveness of the model as shown in Fig. 14. The response predictions are compared with the analysis result by ABAQUS.

Figs. 15 and 16 present the response predictions and the result by ABAQUS. The hysteretic loops of the beam are shown in Fig. 17. As can be seen, the results obtained for the hysteretic response for the deep learning model match closely with the results from ABAQUS. Therefore, the deflection response of a plastic beam can be predicted by the neural network model studied in this paper. This means that the nonlinear hysteretic behavior can be simulated by the Prandtl-Ishlinskii model effectively.

To better illustrate the advantages of proposed method, we regard the result of elastic beam by mode superposition method and result of plastic beam by solid unit model as the exact results. We regard the results of elastic beam by mode superposition method and plastic beam by solid unit model as the exact values. As it is shown in Tab. 1, the proposed method is superior to that of FEM analysis in terms of the computational time and for the same structure and the external load.

Thus, it can be speculated that for the application of this approach, in dealing with more complex and large structures the proposed model should be advantageous.

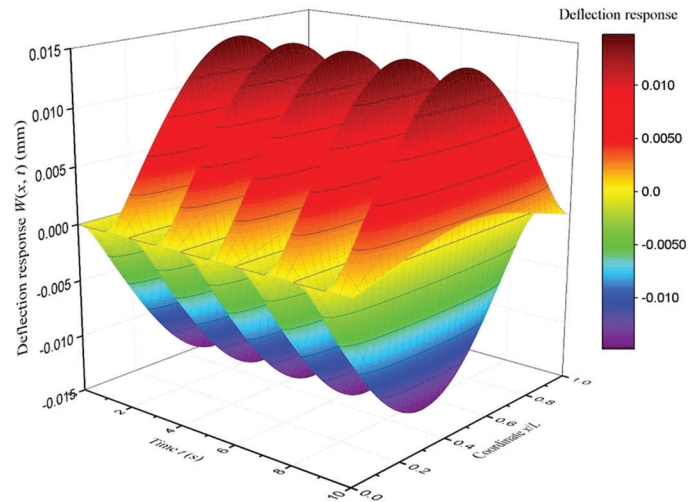


Figure 13: The training data for the response prediction for example 2

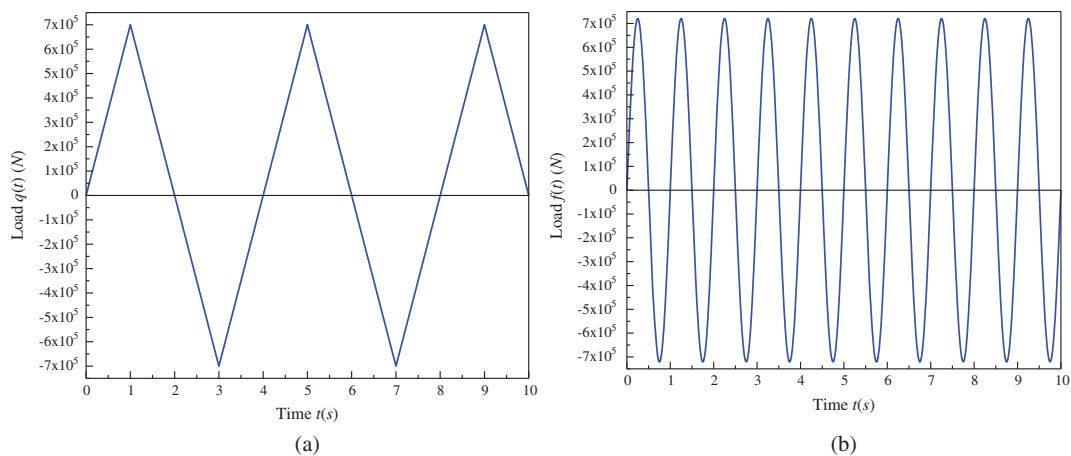


Figure 14: The test load for the verification used in example 2. (a) Triangular periodic load and (b) Harmonic load

The number of chosen points will also influence the response prediction precision. Therefore, we compare the prediction result when the number of selected points are different. As it is presented in Fig. 18, the deflection prediction result of different selected points are compared. In general, the prediction result is closer to the real response with the increase of the number of selected points. However, the more chosen points mean the more undetermined parameter of deep learning model. More training samples are required for neural network training. Because of the limitation of training samples, the chosen point number is usually less than five.

3.3 Vibration of Elastic Continuum Beam under Seismic Load

As it is shown in Fig. 19, a continuous beam subjected to seismic load is considered with the length of beam $L = 15000$ mm. The cross section is rectangular with a height of $h = 300$ mm and a width of $b = 700$ mm. The beam is made of elastic material with density $\rho = 7800$ kg/m³ and elastic modulus $E = 210$ GPa. For building the surrogate model to predict the deflection response of the beam, we will choose five points along the beam as $\{x_1, x_2, x_3, x_4\}$ and the corresponding deflections as

$\{W(x_1, t), W(x_2, t), W(x_3, t), W(x_4, t)\}$. In this example, $x_1 = 0.2L$, $x_2 = 0.4L$, $x_3 = 0.6L$, $x_4 = 0.8L$. We use the deflection response under white noise load as the training data. The white noise data we use to generate the training data is presented in Fig. 20. The trained model is utilized to predict the displacement response under EI Centro earthquake. Fig. 21 shows part of the training data. We use the same deep learning model as in Section 3.1 to predict the displacement response of elastic beams under seismic load. The response predictions are compared with the analytical results by using OpenSees. As it is shown in Fig. 22, the proposed deep learning model can well predict the deflection response of the elastic beam under seismic load.

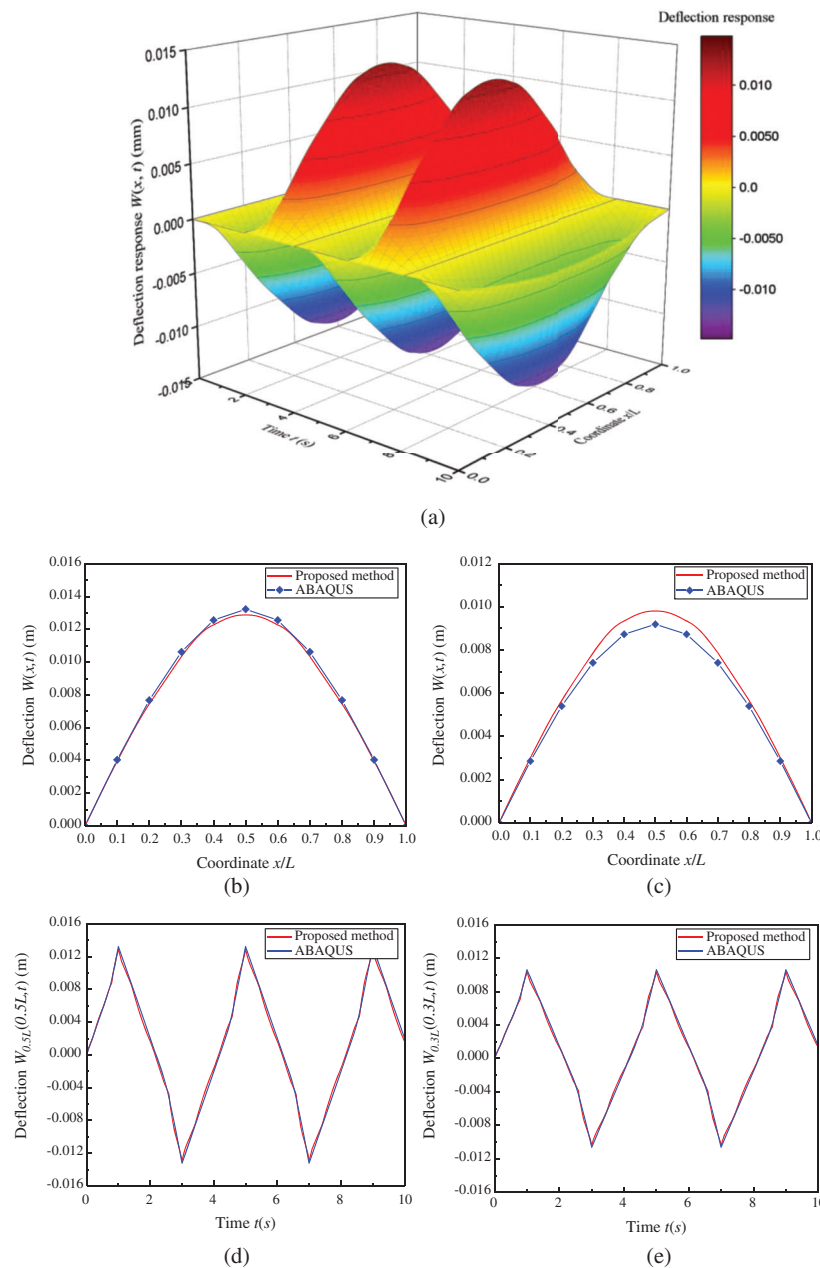


Figure 15: Response prediction of a plastic beam under triangular periodic load. (a) The 3D figures of the beam deflection as a function time t and coordinate x under triangular periodic load, (b) The deflection of beam at $t = 1.0$ s, (c) The deflection of beam at $t = 4.8$ s, (d) The beam deflection $W(0.5L, t)$ and (e) The beam deflection $W(0.3L, t)$

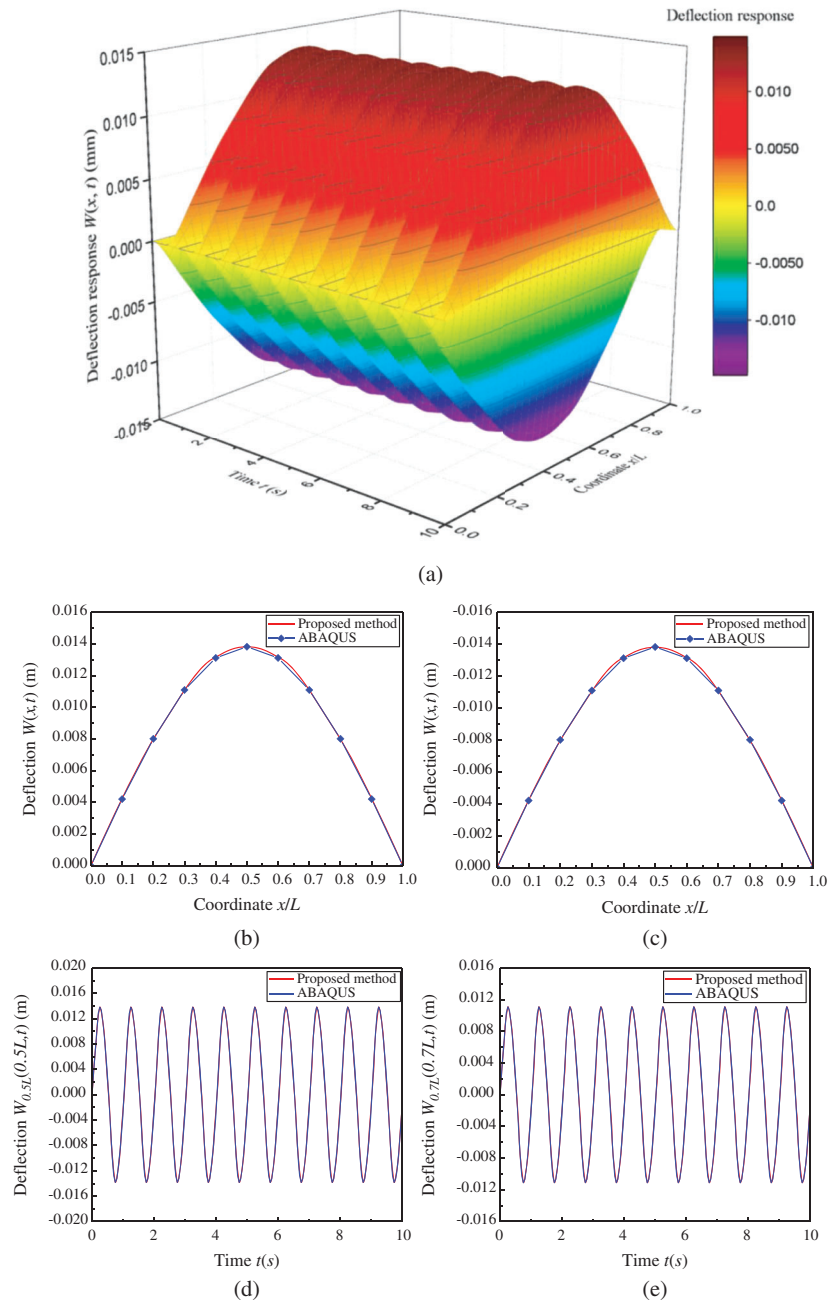


Figure 16: Response prediction of a plastic beam under harmonic load. (a) The 3D plots of the dynamic deflection as a function of time t and coordinate x under rectangular periodic load, (b) The deflection of beam at $t = 0.25$ s, (c) The deflection of beam at $t = 4.75$ s, (d) The beam deflection $W(0.5L, t)$ and (e) The beam deflection $W(0.7L, t)$

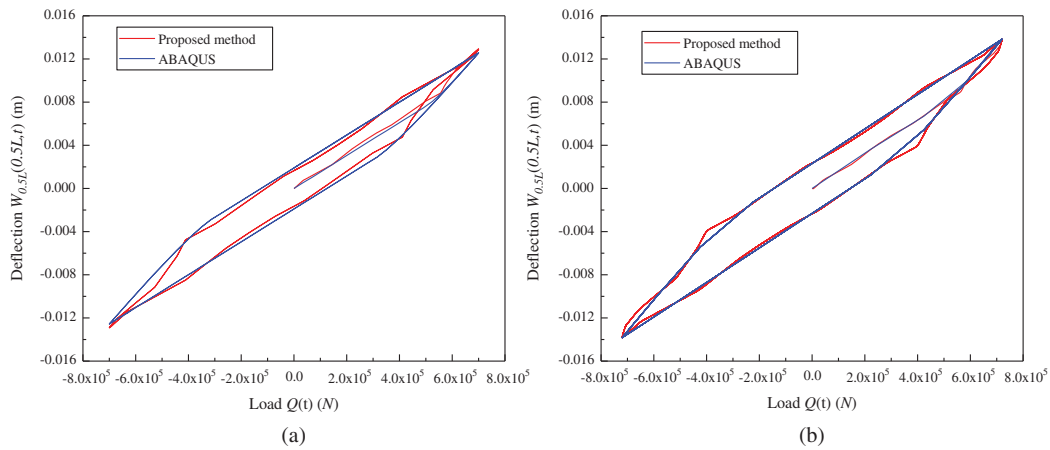


Figure 17: Hysteretic loops of the restoring force for a beam under triangular periodic and harmonic loads. (a) Triangular periodic load and (b) Harmonic load

Table 1: Comparison of calculation time of proposed method and finite element method

Method	Proposed approach (by MATLAB)	ABAQUS (beam element)	ABAQUS (plane stress element)
Linear elastic	0.55 s	71.12 s	120.43 s
Ideal plastic	12.25 s	187.68 s	523.12 s

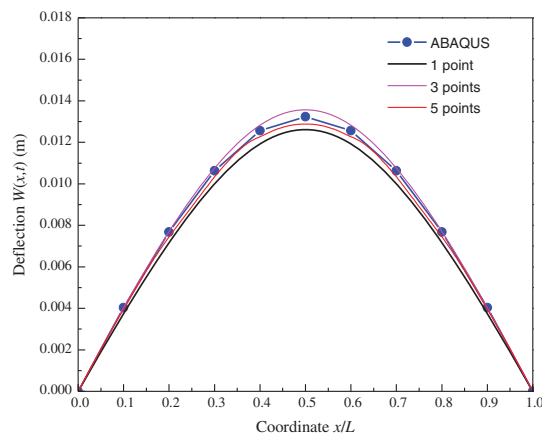


Figure 18: A comparison of deflection prediction of different chosen point at $t = 0.5$ s under triangular periodic load

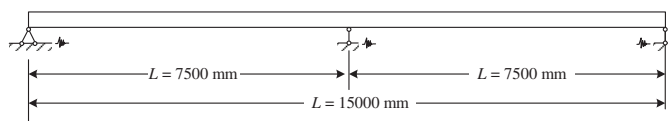


Figure 19: The force diagram of the continue beam under seismic load

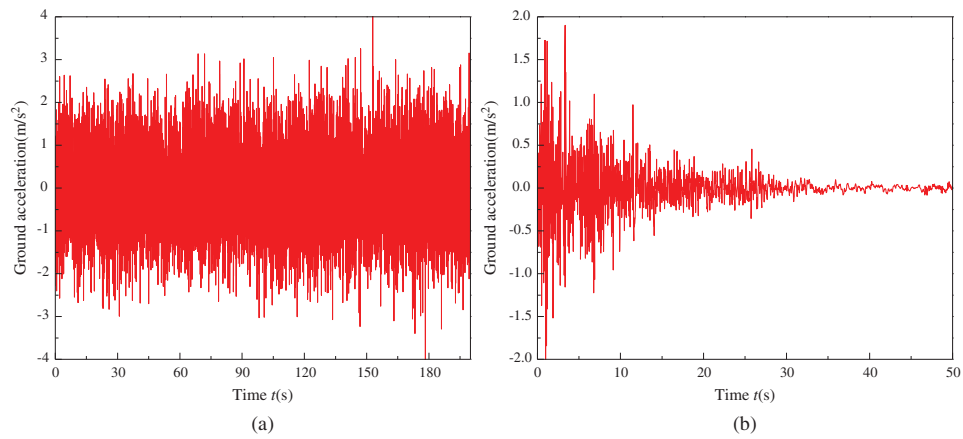


Figure 20: The training and test load for response prediction. (a) Training load- white noise and (b) Test load- EI centro earthquake

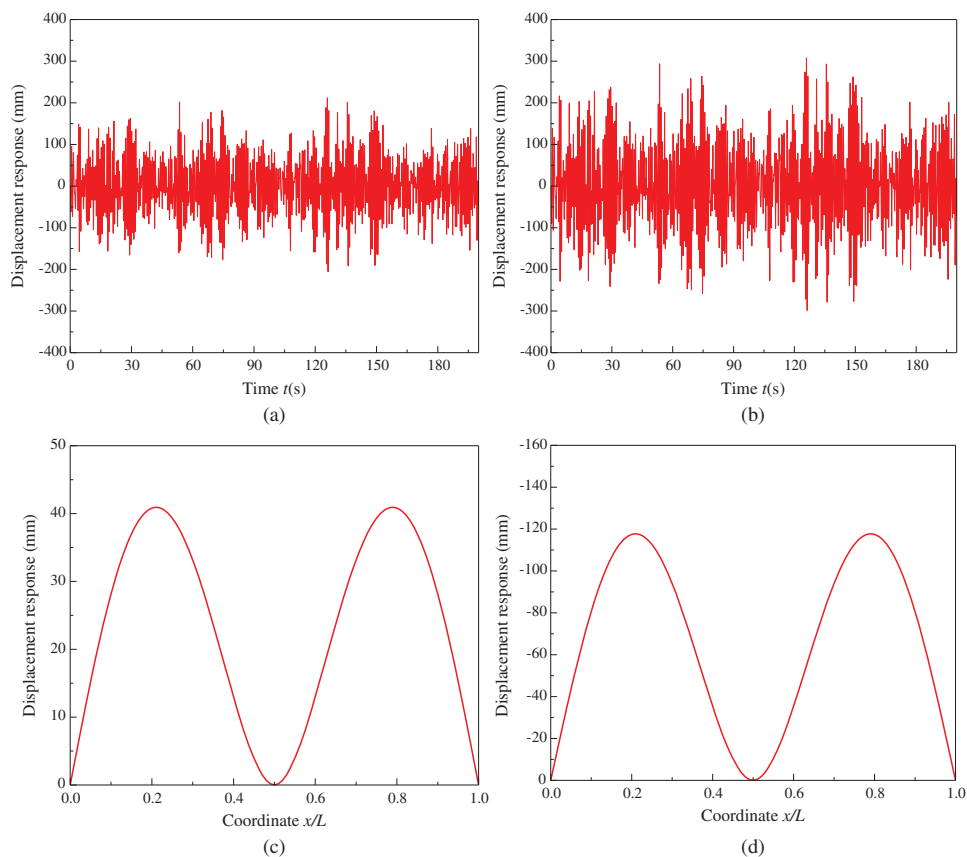


Figure 21: The training displacement response data. (a) Training response of elastic beam $W(0.1L, t)$, (b) Training response of plastic beam $W(0.2L, t)$, (c) Training response of elastic beam at $t = 7.36$ s and (d) Training response of elastic beam at $t = 83.6$ s

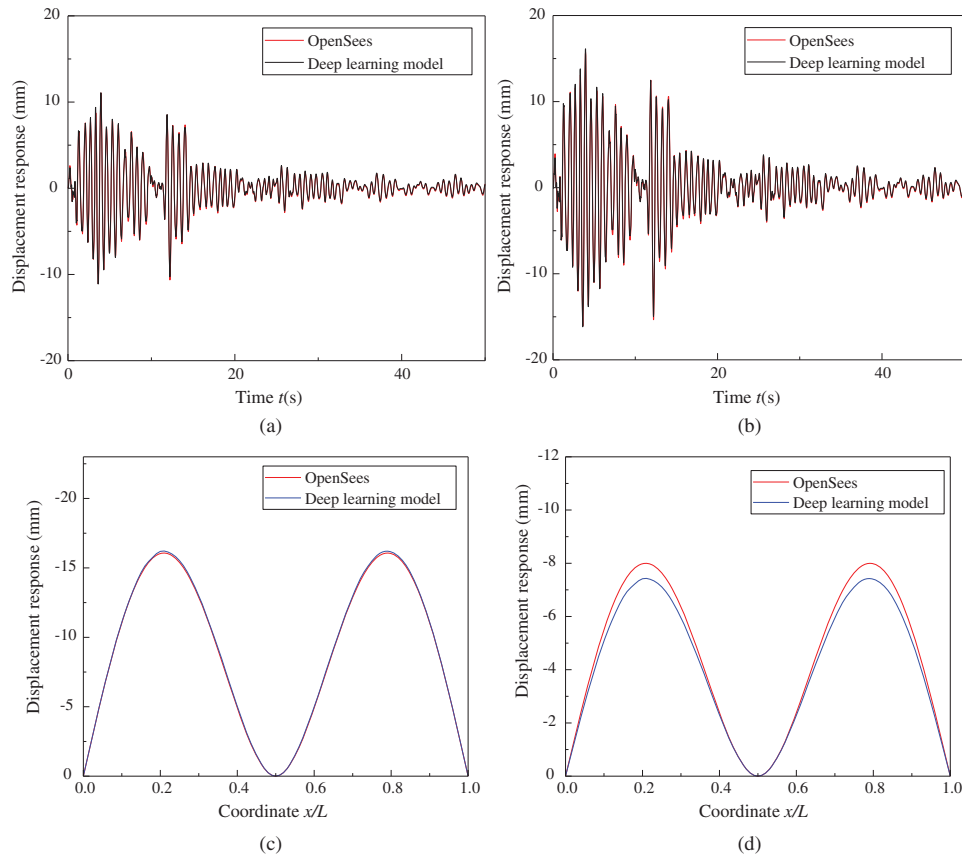


Figure 22: Response prediction of elastic beam under seismic load. (a) Response prediction of elastic beam $W(0.1L, t)$, (b) Response prediction of elastic beam $W(0.2L, t)$, (c) Response prediction of plastic beam at $t = 13.64$ s and (d) Response prediction of plastic beam at $t = 27.92$ s

3.4 Vibration of Plastic Continuous Beam under Seismic Load

In engineering application, a consideration of plastic deformation for beam-like structures is very important in structural design and analysis. Therefore, an example of a plastic continuous beam under seismic load is presented in this section. As in Fig. 19, a continuous beam subjected to seismic load is considered with the length of beam $L = 15000$ mm. The cross section is rectangular with a height of $h = 300$ mm and a width of $b = 700$ mm. The beam is made of an ideal plastic material with density $\rho = 7800$ kg/m³, elastic modulus $E = 210$ GPa and yield strength $f_y = 335$ Mpa. We choose five points along the beam as $\{x_1, x_2, x_3, x_4\}$ and the corresponding deflections as $\{W(x_1, t), W(x_2, t), W(x_3, t), W(x_4, t)\}$. In this example, $x_1 = 0.2L$, $x_2 = 0.4L$, $x_3 = 0.6L$, $x_4 = 0.8L$.

As shown in Fig. 23, a seismic load is used to generate the training data. The trained model is utilized to predict the displacement response under EI Centro earthquake. Fig. 24 shows part of the training data. The deep learning model to predict the displacement response of plastic beam under seismic load has the same architecture as the model in Section 3.2. As shown in Fig. 25, the proposed deep learning model can predict the deflection response of the plastic beam under seismic load. However, due to the error caused by Prandtl-Ishlinskii model, the prediction has a lower but acceptable accuracy.

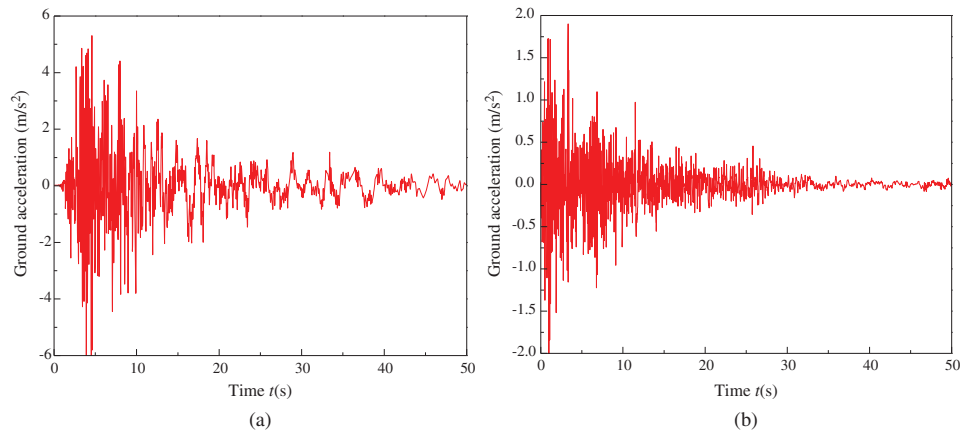


Figure 23: The training and test load for response prediction. (a) Training load and (b) Test load

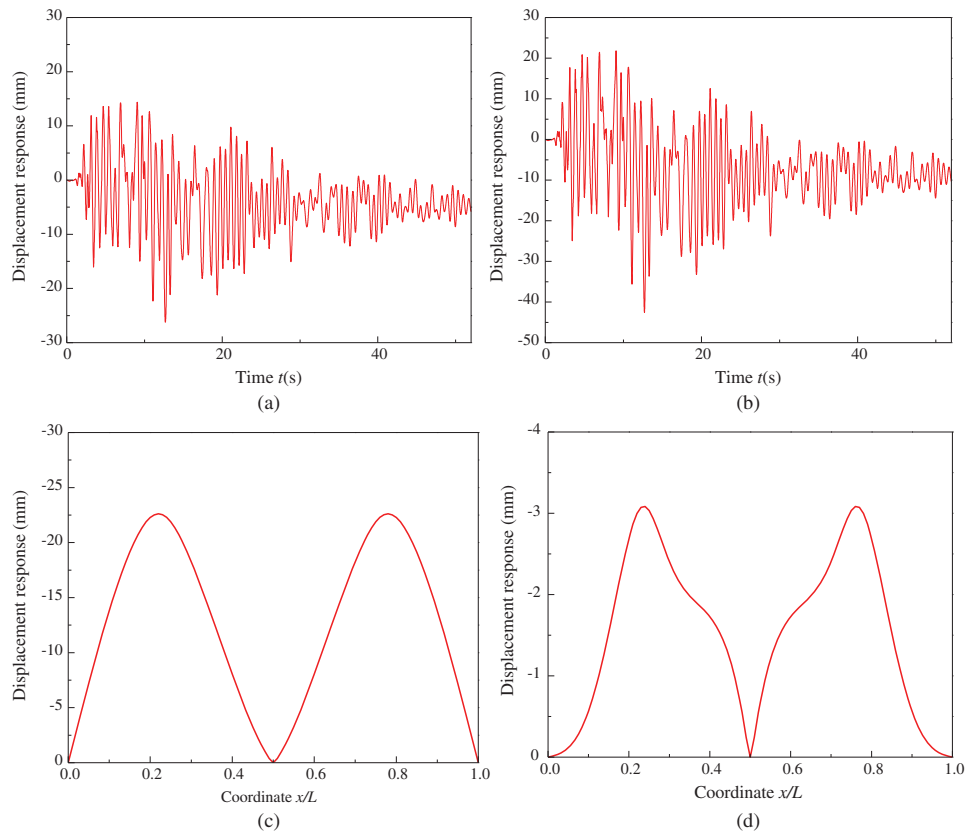


Figure 24: The training displacement response data of plastic beam. (a) Training response of elastic beam $W(0.1L, t)$, (b) Training response of elastic beam $W(0.2L, t)$, (c) Training response of elastic beam at $t = 20.80$ s and (d) Training response of elastic beam at $t = 41.53$ s

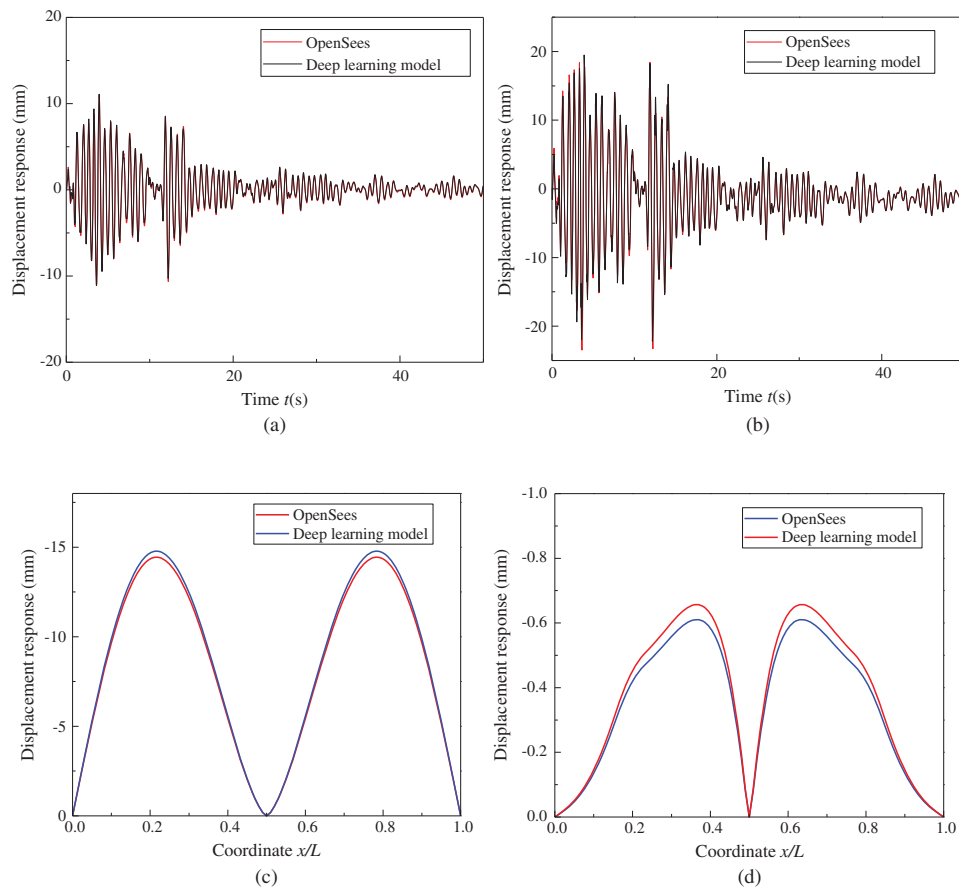


Figure 25: Response prediction of elastic beam under seismic load. (a) Response prediction of elastic beam $W(0.1L, t)$, (b) Response prediction of elastic beam $W(0.2L, t)$, (c) Response prediction of elastic beam at $t = 3.64$ s and (d) Response prediction of elastic beam at $t = 7.92$ s

4 Conclusions

Based on the governing partial differential equation of Euler-Bernoulli beam, a deep learning surrogate model for the deflection response prediction of beam-like structures is proposed. The model can be divided into two sub-networks. The first network (ANN-1) approximates the shape function of the beam by deep neural network while the second one (ANN-2) is a feedback neural network which can predict the displacement and the velocity response at each reference point. The beams made of both elastic and plastic materials are analyzed by using Prandtl-Ishlinskii model to simulate the hysteresis of the structure.

Four numerical examples are presented to validate the effectiveness of the proposed approach. The example shown in Section 3.1 is a surrogate model of the elastic beam which uses the training data from mode superposition method, and the predicted results are compared with the Newmark- β method. The second example considers the material's plasticity. Training data are generated by ABAQUS. The third and fourth examples aim to simulate the seismic response prediction of elastic and plastic beam. The following conclusions can be drawn from the results:

1. The proposed deep learning based model can well predict the deflection response of an elastic and a plastic beam structure.

2. Compared with the elastic beam, there will be a bigger error when the nonlinear vibration of the plastic beam is predicted by the proposed approach. Even so, the prediction result is still acceptable.
3. The hysteresis of the structure that represents the plasticity can be simulated by the Prandtl-Ishlinskii model which is embedded in the deep learning model and the hysteresis loop can be approximated.
4. The proposed method runs much faster than the conventional finite element method, in terms of the computational time. Therefore, the proposed method has some advantages in practical engineering problems.
5. The proposed method can be used for the seismic response prediction of beam-like structure. And describe the vibration shape of both elastic and plastic beam. It will help in the seismic analysis of bridge structure. Application of the proposed approach for more analyzing the dynamic response of more complex problems needs to be investigated.

Funding Statement: The author(s) received no specific funding for this study.

Conflicts of Interest: The author(s) declare no potential conflicts of interest with respect to the research, authorship, and/or publication of this article.

References

1. Bjorhovde, R., Ravindra, M., Galambos, T. (1978). LRFD criteria for steel beam-columns. *Structural Division, 104(9)*, 1371–1387.
2. Fujikake, K., Bing, L., Sam, S. (2009). Impact response of reinforced concrete beam and its analytical evaluation. *Journal of Structural Engineering, 135(8)*, 938–950. DOI 10.1061/(ASCE)ST.1943-541X.0000039.
3. Marti, P. (1985). Basic tools of reinforced concrete beam design. *Proceedings, 82(1)*, 46–56.
4. Zhao, Y., Noori, M., Altabey, W. A. (2017). Damage detection for a beam under transient excitation via three different algorithms. *Structural Engineering and Mechanics, 64(6)*, 803–817. DOI 10.12989/sem.2017.64.6.803.
5. Zhao, Y., Noori, M., Altabey, W. A., Seyed, B. B. (2018). Mode shape based damage identification for a reinforced concrete beam using wavelet coefficient differences and multiresolution analysis. *Structural Control and Health Monitoring, 25(1)*, e2041. DOI 10.1002/stc.2041.
6. Zhao, Y., Noori, M., Altabey, W. A., Awad, T. (2019). A comparison of three different methods for the identification of hysterically degrading structures using BWBN model. *Frontiers in Built Environment, 4(80)*, 1–19. DOI 10.3389/fbuil.2018.00080.
7. Silik, A., Noori, M., Altabey, W. A., Ghiasi, R. (2020). Comparative analysis of wavelet transform for time-frequency analysis and transient localization in structural health monitoring. *Structural Durability & Health Monitoring* (In Press). <http://www.tpsubmission.com/index.php/sdhm>.
8. Silik, A., Noori, M., Altabey, W. A., Ghiasi, R. (2020). Choosing Optimum levels of wavelet multi-resolution analysis for time-varying signals in structural health monitoring. *Structural Control and Health Monitoring* (In Press). <https://onlinelibrary.wiley.com/journal/15452263>.
9. Li, Z., Noori, M., Altabey, W. A. (2020). An experimental study on the seismic performance of adobe walls. *Structural Durability & Health Monitoring* (In Press). <http://www.tpsubmission.com/index.php/sdhm>.
10. Apuzzo, A., Barretta, R., Luciano, R., Francesco, M. D., Rosa, P. (2017). Free vibrations of Bernoulli-Euler nano-beams by the stress-driven nonlocal integral model. *Composites Part B: Engineering, 123*, 105–111. DOI 10.1016/j.compositesb.2017.03.057.
11. Mahmoudpour, E., Hosseini-Hashemi, S. H., Faghidian, S. A. (2018). Nonlinear vibration analysis of FG nano-beams resting on elastic foundation in thermal environment using stress-driven nonlocal integral model. *Applied Mathematical Modelling, 57*, 302–315. DOI 10.1016/j.apm.2018.01.021.
12. Altabey, W. A. (2017). An exact solution for mechanical behavior of BFRP Nano-thin films embedded in NEMS. *Advances in Nano Research, 5(4)*, 337–357. DOI 10.12989/anr.2017.5.4.337.
13. Altabey, W. A., Noori, M., Alarjani, A., Zhao, Y. (2020). Nano-delamination monitoring of BFRP nano-pipes of electrical potential change with ANNs. *Advances in Nano Research, 9(1)*, 1–13. DOI 10.12989/anr.2020.9.1.001.

14. Wang, T., Noori, M., Altabay, W. A. (2020). Identification of cracks in an Euler–Bernoulli beam using Bayesian inference and closed-form solution of vibration modes. *Proceedings of the Institution of Mechanical Engineers, Part L: Journal of Materials: Design and Applications*, DOI 10.1177/1464420720969719.
15. Sherafatnia, K., Farrahi, G., Faghidian, S. A. (2014). Analytic approach to free vibration and buckling analysis of functionally graded beams with edge cracks using four engineering beam theories. *International Journal of Engineering*, 27(6), 979–990.
16. Hag-Elsafi, O., Alampalli, S., Kunin, J. (2001). Application of FRP laminates for strengthening of a reinforced-concrete T-beam bridge structure. *Composite Structures*, 52(3–4), 453–466. DOI 10.1016/S0263-8223(01)00035-6.
17. Noori, M., Wang, H., Altabay, W. A., Silik, A. I. H. (2018). A modified wavelet energy rate based damage identification method for steel bridges. *Scientia Iranica, Transactions B: Mechanical Engineering*, 25(6), 3210–3230. DOI 10.24200/sci.2018.20736.
18. Altabay, W. A. (2017). Free vibration of basalt fiber reinforced polymer (FRP) laminated variable thickness plates with intermediate elastic support using finite strip transition matrix (FSTM) method. *Journal of Vibroengineering*, 19(4), 2873–2885. DOI 10.21595/jve.2017.18154.
19. Altabay, W. A. (2017). Prediction of natural frequency of basalt fiber reinforced polymer (FRP) laminated variable thickness plates with intermediate elastic support using artificial neural networks (ANNs) method. *Journal of Vibroengineering*, 19(5), 3668–3678. DOI 10.21595/jve.2017.18209.
20. Altabay, W. A. (2018). High performance estimations of natural frequency of basalt FRP laminated plates with intermediate elastic support using response surfaces method. *Journal of Vibroengineering*, 20(2), 1099–1107. DOI 10.21595/jve.2017.18456.
21. Zhao, Y., Noori, M., Altabay, W. A. (2020). Reaching law based sliding mode control for a frame structure under seismic load. *Earthquake Engineering and Engineering Vibration* (In Press). <http://https://www.springer.com/journal/11803>.
22. Wilson, J. (2003). Earthquake response of tall reinforced concrete chimneys. *Engineering Structures*, 25(1), 11–24. DOI 10.1016/S0141-0296(02)00098-6.
23. Wang, A., Lin, Y. (2007). Vibration control of a tall building subjected to earthquake excitation. *Journal of Sound and Vibration*, 299(4–5), 757–773. DOI 10.1016/j.jsv.2006.07.016.
24. Mack, Y., Goel, T., Shyy, W., Haftka, R. (2007). *Surrogate model-based optimization framework: a case study in aerospace design, Evolutionary computation in dynamic and uncertain environments*, 323–342. Berlin, Heidelberg: Springer.
25. Han, Z., Zhang, K. (2012). Surrogate-based optimization. *Real-World Applications of Genetic Algorithms*, 343–362.
26. Altabay, W. A. (2017). A study on thermo-mechanical behavior of MCD through bulge test analysis. *Advances in Computational Design*, 2(2), 107–119. DOI 10.12989/acd.2017.2.2.107.
27. Ghannadi, P., Kourehli, S. S., Noori, M., Altabay, W. A. (2020). Efficiency of grey wolf optimization algorithm for damage detection of skeletal structures via expanded mode shapes. *Advances in Structural Engineering*, 23(13), 2850–2865. DOI 10.1177/1369433220921000.
28. Choi, S., Grandhi, R., Canfield, R. (2004). Structural reliability under non-Gaussian stochastic behavior. *Computers & structures*, 82(13–14), 1113–1121. DOI 10.1016/j.compstruc.2004.03.015.
29. Su, G., Peng, L., Hu, L. (2017). A Gaussian process-based dynamic surrogate model for complex engineering structural reliability analysis. *Structural Safety*, 68, 97–109. DOI 10.1016/j.strusafe.2017.06.003.
30. Kang, F., Xu, Q., Li, J. (2016). Slope reliability analysis using surrogate models via new support vector machines with swarm intelligence. *Applied Mathematical Modelling*, 40(11–12), 6105–6120. DOI 10.1016/j.apm.2016.01.050.
31. Zhao, Y., Noori, M., Altabay, W. A., Naiwei, L. (2017). Reliability evaluation of a laminate composite plate under distributed pressure using a hybrid response surface method. *International Journal of Reliability, Quality and Safety Engineering*, 24(3), 1750013. DOI 10.1142/S0218539317500139.

32. Gao, H., Guo, X., Hu, X. (2012). Crack identification based on Kriging surrogate model. *Structural Engineering and Mechanics*, 41(1), 25–41. DOI 10.12989/sem.2012.41.1.025.
33. Torkzadeh, P., Fathnejat, H., Ghiasi, R. (2016). Damage detection of plate-like structures using intelligent surrogate model. *Smart Structures and Systems*, 18(6), 1233–1250. DOI 10.12989/sss.2016.18.6.1233.
34. Ghasemi, M. R., Ghiasi, R., Varae, H. (2017). Probability-based damage detection of structures using surrogate model and enhanced ideal gas molecular movement algorithm. *World Congress of Structural and Multidisciplinary Optimisation*, 1657–1674. Cham: Springer,
35. Zhao, Y., Noori, M., Altabay, W. A., Wu, Z. (2018). Fatigue damage identification for composite pipeline systems using electrical capacitance sensors. *Smart Materials and Structures*, 27(8), 085023. DOI 10.1088/1361-665X/aacc99.
36. Zhao, Y., Noori, M., Altabay, W. A., Ramin, G., Wu, Z. (2019). A fatigue damage model for FRP composite laminate systems based on stiffness reduction. *Structural Durability & Health Monitoring*, 13(1), 85–103. DOI 10.32604/sdhm.2019.04695.
37. Altabay, W. A. (2017). Delamination evaluation on basalt FRP composite pipe of electrical potential change. *Advances in Aircraft and Spacecraft Science*, 4(5), 515–528. DOI 10.12989/aas.2017.4.5.515.
38. Altabay, W. A. (2017). EPC method for delamination assessment of basalt FRP pipe: Electrodes number effect. *Structural Monitoring and Maintenance*, 4(1), 69–84. DOI 10.12989/smm.2017.4.1.069.
39. Altabay, W. A., Noori, M. (2017). Detection of fatigue crack in basalt FRP laminate composite pipe using electrical potential change method. *12th International Conference on Damage Assessment of Structures, IOP Conference Series: Journal of Physics*, 842, 012079.
40. Altabay, W. A., Noori, M. (2018). Fatigue life prediction for carbon fibre/epoxy laminate composites under spectrum loading using two different neural network architectures. *International Journal of Sustainable Materials and Structural Systems (IJSMSS)*, 3(1), 53–78. DOI 10.1504/IJSMSS.2017.10013394.
41. Altabay, W. A. (2016). The thermal effect on electrical capacitance sensor for two-phase flow monitoring. *Structural Monitoring and Maintenance*, 3(4), 335–347. DOI 10.12989/smm.2016.3.4.335.
42. Altabay, W. A., Noori, M. (2018). Monitoring the water absorption in GFRE pipes via an electrical capacitance sensors. *Advances in Aircraft and Spacecraft Science*, 5(4), 411–434. DOI 10.12989/aas.2018.5.4.411.
43. Altabay, W. A., Noori, M., Alarjani, A., Zhao, Y. (2020). Tensile creep monitoring of basalt fiber reinforced polymers plates via electrical potential change and artificial neural network. *Scientia Iranica, Transactions B: Mechanical Engineering*, 27(4), 1995–2008. DOI 10.24200/SCI.2020.52754.2874.
44. Ghiasi, R., Ghasemi, M. R., Noori, M., Altabay, W. A. (2019). A non-parametric approach toward structural health monitoring for processing big data collected from the sensor network. *Structural Health Monitoring 2019: Enabling Intelligent Life-Cycle Health Management for Industry Internet of Things (IIOT). Proceedings of the 12th International Workshop on Structural Health Monitoring (IWSHM 2019)*. Stanford, California, USA.
45. Hosder, S., Watson, L., Grossman, B., Mason, W. H., Kim, H. et al. (2001). Polynomial response surface approximations for the multidisciplinary design optimization of a high speed civil transport. *Optimization and Engineering*, 2(4), 431–452. DOI 10.1023/A:1016094522761.
46. Venkatesh, V., Goyal, S. (2010). Expectation disconfirmation and technology adoption: Polynomial modeling and response surface analysis. *MIS Quarterly*, 34(2), 281–303. DOI 10.2307/20721428.
47. Han, Z., Görtz, S. (2012). Hierarchical Kriging model for variable-fidelity surrogate modeling. *AIAA Journal*, 50(9), 1885–1896. DOI 10.2514/1.J051354.
48. Kleijnen, J. (2009). Kriging metamodeling in simulation: A review. *European Journal of Operational Research*, 192(3), 707–716. DOI 10.1016/j.ejor.2007.10.013.
49. Kaymaz, I. (2005). Application of kriging method to structural reliability problems. *Structural Safety*, 27(2), 133–151. DOI 10.1016/j.strusafe.2004.09.001.
50. Sreekanth, J., Datta, B. (2010). Multi-objective management of saltwater intrusion in coastal aquifers using genetic programming and modular neural network based surrogate models. *Journal of Hydrology*, 393(3–4), 245–256. DOI 10.1016/j.jhydrol.2010.08.023.

51. Melo, A. P., Cóstola, D., Lamberts, R., Hensen, J. L. M. (2014). Development of surrogate models using artificial neural network for building shell energy labelling. *Energy Policy*, 69, 457–466. DOI 10.1016/j.enpol.2014.02.001.
52. Manik, A., Gopalakrishnan, K., Singh, A., Yan, S. (2008). Neural networks surrogate models for simulating payment risk in pavement construction. *Journal of Civil Engineering and Management*, 14(4), 235–240. DOI 10.3846/1392-3730.2008.14.22.
53. Altabay, W. A. (2016). FE and ANN model of ECS to simulate the pipelines suffer from internal corrosion. *Structural Monitoring and Maintenance*, 3(3), 297–314. DOI 10.12989/smm.2016.3.3.297.
54. Altabay, W. A. (2016). Detecting and predicting the crude oil type inside composite pipes using ECS and ANN. *Structural Monitoring and Maintenance*, 3(4), 377–393. DOI 10.12989/smm.2016.3.4.377.
55. Zhao, Y., Noori, M., Altabay, W. A., Ghiasi, R., Zhishen, W. (2018). Deep learning-based damage, load and support identification for a composite pipeline by extracting modal macro strains from dynamic excitations. *Applied Sciences*, 8(12), 2564. DOI 10.3390/app8122564.
56. Kost, A., Altabay, W. A., Noori, M., Awad, T. (2019). Applying neural networks for tire pressure monitoring systems. *Structural Durability & Health Monitoring*, 13(3), 247–266. DOI 10.32604/sdhm.2019.07025.
57. Hornik, K., Stinchcombe, M., White, H. (1989). Multilayer feedforward networks are universal approximators. *Neural Networks*, 2(5), 359–366. DOI 10.1016/0893-6080(89)90020-8.
58. Hornik, K. (1991). Approximation capabilities of multilayer feedforward networks. *Neural Networks*, 4(2), 251–257. DOI 10.1016/0893-6080(91)90009-T.
59. Masri, S., Chassiakos, A., Caughey, T. (1993). Identification of nonlinear dynamic systems using neural networks. *Journal of Applied Mechanics*, 60(1), 123–133. DOI 10.1115/1.2900734.
60. He, Y., Hu, X., Zhan, S. (1996). Predicting seismic response of structure by artificial neural network. *Transactions of Tianjin University*, (2), 36–39.
61. He, Y., Wu, J. (1998). Prediction of structural response by self-recurrent neural network. *China Civil Engineering Journal*, 2, 46–51 (In Chinese).
62. Wu, J., He, Y. (2000). The new achievements of neural network's application in structural vibration control. *World Information on Earthquake Engineering*, 16, 10–19 (In Chinese).
63. Joghataie, A., Farrokh, M. (2008). Dynamic analysis of nonlinear frames by Prandtl neural networks. *Journal of Engineering Mechanics*, 134(11), 961–969. DOI 10.1061/(ASCE)0733-9399(2008)134:11(961).
64. Brokate, M., Sprekels, J. (2012). *Hysteresis and phase transitions*. Berlin. Springer Science & Business Media.
65. Lagaros, N., Papadrakakis, M. (2012). Neural network based prediction schemes of the non-linear seismic response of 3D buildings. *Advances in Engineering Software*, 44(1), 92–115. DOI 10.1016/j.advengsoft.2011.05.033.
66. LeCun, Y., Bengio, Y., Hinton, G. (2016). Deep learning. *Nature*, 521(7553), 436–444. DOI 10.1038/nature14539.
67. Goodfellow, I., Bengio, Y., Courville, A. (2016). *Deep learning*. Massachusetts, USA: MIT Press.
68. Zhang, R., Chen, Z., Chen, S., Zheng, J., Büyüköztürk, O. et al. (2019). Deep long short-term memory networks for nonlinear structural seismic response prediction. *Computers & Structures*, 220, 55–68. DOI 10.1016/j.compstruc.2019.05.006.
69. Ljung, L. (2001). Black-box models from input-output measurements//IMTC 2001. *Proceedings of the 18th IEEE Instrumentation and Measurement Technology Conference, Rediscovering measurement in the age of informatics (Cat. No. 01CH 37188)*, vol. 1, 138–146. Budapest, IEEE.
70. Yadav, N., Yadav, A., Kumar, M. (2015). *An introduction to neural network methods for differential equations*. Netherlands: Springer.
71. He, S., Reif, K., Unbehauen, R. (2000). Multilayer neural networks for solving a class of partial differential equations. *Journal of Neural Networks*, 13(3), 385–396. DOI 10.1016/S0893-6080(00)00013-7.
72. Mai-Duy, N., Tran-Cong, T. (2003). Approximation of function and its derivatives using radial basis function networks. *Applied Mathematical Modelling*, 27(3), 197–220. DOI 10.1016/S0307-904X(02)00101-4.
73. Kumar, M., Yadav, N. (2013). Buckling analysis of a beam–column using multilayer perceptron neural network technique. *Journal of the Franklin Institute*, 350(10), 3188–3204. DOI 10.1016/j.jfranklin.2013.07.016.

74. Takeuchi, J., Kosugi, Y. (1994). Neural network representation of finite element method. *Neural Networks*, 7(2), 389–395. DOI 10.1016/0893-6080(94)90031-0.
75. Han, J., Jentzen, A., Weinan, E. (2018). Solving high-dimensional partial differential equations using deep learning. *Proceedings of the National Academy of Sciences of The United States of America*, 115(34), 8505–8510. DOI 10.1073/pnas.1718942115.
76. Sirignano, J., Spiliopoulos, K. (2018). DGM: A deep learning algorithm for solving partial differential equations. *Journal of Computational Physics*, 375, 1339–1364. DOI 10.1016/j.jcp.2018.08.029.
77. Wang, J., Wu, J., Xiao, H. (2017). Physics-informed machine learning approach for reconstructing Reynolds stress modeling discrepancies based on DNS data. *Physical Review Fluids*, 2(3), 034603. DOI 10.1103/PhysRevFluids.2.034603.
78. Wu, J., Xiao, H., Paterson, E. (2018). Physics-informed machine learning approach for augmenting turbulence models: A comprehensive framework. *Physical Review Fluids*, 3(7), 074602. DOI 10.1103/PhysRevFluids.3.074602.
79. Wu, J., Sun, R., Laizet, S., Xiao, H. (2019). Representation of stress tensor perturbations with application in machine-learning-assisted turbulence modeling. *Computer Methods in Applied Mechanics and Engineering*, 346, 707–726. DOI 10.1016/j.cma.2018.09.010.
80. Raissi, M., Perdikaris, P., Karniadakis, G. (2017). Physics informed deep learning (Part I): Data-driven solutions of nonlinear partial differential equations. *Artificial Intelligence*, arXiv: 1711.10561.
81. Raissi, M., Perdikaris, P., Karniadakis, G. (2017). Physics informed deep learning (Part II): Data-driven discovery of nonlinear partial differential equations. *Artificial Intelligence*, arXiv: 1711.10566.
82. Raissi, M., Karniadakis, G. (2018). Hidden physics models: Machine learning of nonlinear partial differential equations. *Journal of Computational Physics*, 357, 125–141. DOI 10.1016/j.jcp.2017.11.039.
83. Raissi, M. (2018). Deep hidden physics models: Deep learning of nonlinear partial differential equations. *Journal of Machine Learning Research*, 19(1), 932–955.
84. Raissi, M., Wang, Z., Triantafyllou, M., Karniadakis, G. E. (2019). Deep learning of vortex-induced vibrations. *Journal of Fluid Mechanics*, 861, 119–137. DOI 10.1017/jfm.2018.872.
85. Griewank, A., Walther, A. (2003). Introduction to automatic differentiation. *Proceedings in Applied Mathematics and Mechanics*, 2(1), 45–49. Berlin: WILEY-VCH Verlag.
86. Butcher, J. (1987). *The numerical analysis of ordinary differential equations: Runge-Kutta and general linear methods*. New York: Wiley.
87. Serpico, C., Visone, C. (1998). Magnetic hysteresis modeling via feed-forward neural networks. *IEEE Transactions on Magnetics*, 34(3), 623–628. DOI 10.1109/20.668055.